Lessons Learnt from HY-2B RFI Activities and Preliminary Studies on RFI Detection and Localization for the Chinese Ocean Salinity Satellite

Yinan Li(1), He Ren(1), Congcong Wang(1), Wu Zhou(2), Wenyu Gao(1)
(1) China Academy of Space Technology (Xi'an), Xi'an 710100, China
(2) National Satellite Ocean Application Service, Beijing 100081, China

Abstract

Distributed from L to high frequency band, Radio frequency interferences (RFIs) are contaminating the geophysical parameters estimated from the measurements of microwave radiometers. Chinese researchers are developing series of Earth observation satellites focusing on the marine dynamic environment for numerical weather prediction and climate monitoring. The scanning microwave radiometer onboard HY-2B (Haiyang-2B) has been monitoring sea surface temperature observations since 2018. After more than 2 years in orbit, an overview of RFI scenario worldwide has been provided and lessons have been learnt from HY-2B RFI activities. The Interferometric Microwave Radiometer (IMR) will be a main payload onboard the Chinese Ocean Salinity Satellite. Preliminary studies have been carried out on RFI detection and localization to improve the performance of this mission.

1 Introduction

The HY-2B mission is one of the Chinese series of Earth observation satellites focusing on the marine dynamic environment. One of the payloads carried by HY-2B satellite is a conical scanning microwave radiometer operating between C to Ka band, which has monitored sea surface temperature since 2018.

As soon as HY-2B data analysis began, it became clear that man-made sources are jeopardizing scientific retrieval of brightness temperature (Tb) in certain areas of the world. Detecting and flagging contaminated observations present a continuous challenge. A robust method of detecting RFI based on spectral difference has been carried out to improve the quality of brightness temperature.

The Chinese Ocean Salinity Satellite is an on-going mission aims at monitoring global sea-surface salinity (SSS). The Interferometric Microwave Radiometer (IMR) will be one of the main payloads onboard, which consists of a Y-shaped antenna array with 56 feed elements working at L band [1].

Past experience of SMOS has told us, that even though the instrument works at protected band, the mission will still be influenced by RFI. Low RFI emissions are difficult to detect, but still leading to incorrect physical retrieval. Strong RFI emissions influence large areas through the secondary lobe tails, thus leading to a significant data loss [2]. Therefore, RFI detection is a key step for users to decide whether to keep or discard the snapshot, while localization helps to switch off illegal transmissions.

Current method used to detect RFI in HY-2B mission and lessons learnt from HY-2B RFI activities are shown in Section 2. The detecting method based on statistical characteristics and a precise way to localize RFI sources for the Chinese Ocean Salinity Satellite are introduced in Section 3.

2 Current RFI detecting method in HY-2B

The scanning microwave radiometer of HY-2B works at several frequency bands, including C, X, K and Ka. The measurements are influenced by man-made sources since C and X bands are extensively used for broadcasting. The correlation between brightness temperature at two relatively close frequencies can be used to detect RFI.

2.1 RFI in C band

Measurements at C band are influenced by RFI when observing the earth as well as the cold swath. Differences between co-polar brightness temperature measurements at C and X band are used to detect RFI [3].

$$Index_6 = Tb_{10V} - Tb_{6V} \tag{1}$$

where Tb_{10V} is the brightness temperature centered at 10.65GHz, and Tb_{6V} is the brightness temperature centered at 6.925GHz. RFI is detected when $Index_6$ is smaller than -30K. Fig.1 shows the map of $Index_6$ derived from HY-2B. RFI appears over continental areas in Asia, America, Africa and Australia, as shown in Figure 1 from yellow to blue.

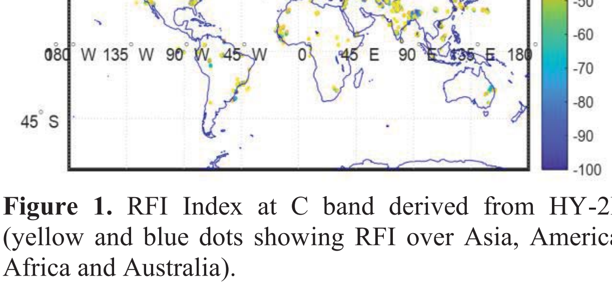

Figure 1. RFI Index at C band derived from HY-2B (yellow and blue dots showing RFI over Asia, America, Africa and Australia).

Figure 2 illustrates the variations of cold view voltage with the latitude. Outliers circled with dotted line shows RFI events occur in regions of northern hemisphere over circumpolar latitude. These events are due to direct broadcasting satellite signals into cold beams.

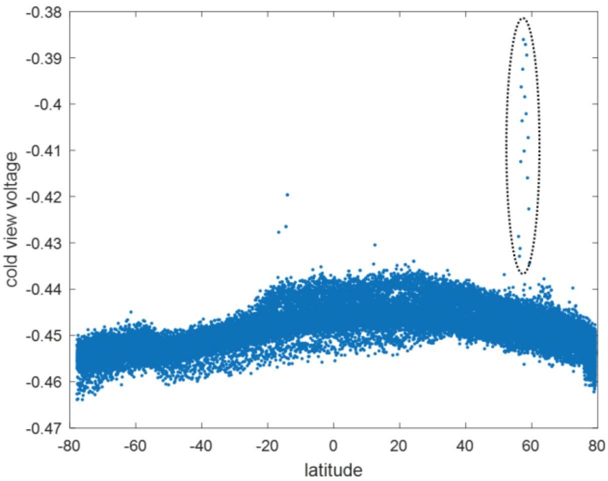

Figure 2. HY-2B RFI at C band in cold view (outliers circled with dotted line showing RFI at around 60°S).

2.2 RFI in K band

Two methods are used to detect RFI in K band [4,5]:

1) Calculate a linear combination of all channels of different frequencies and their squares, then subtract the combination from the channel of interest.

$$\Delta Tb(i) = Tb(i) - \left\{ a_0(i) + \sum \left[a_j(i) Tb(j) + b_j(i) Tb^2(j) \right] \right\} \quad (2)$$

where i represents the channel index to the channel of interest and j is the channel index to all other channels with different center frequency. $\Delta Tb(i)$ is called the generalized RFI index. Figure 3 shows the map of ΔTb centered at 18.7GHz.

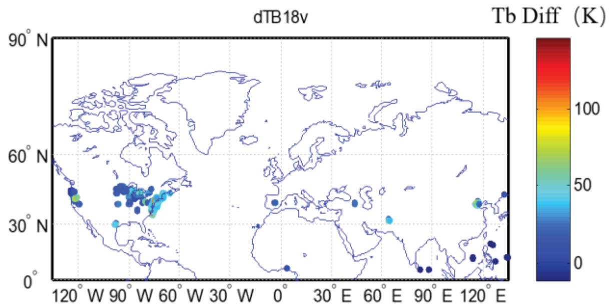

Figure 3. RFI Index at K band derived from HY-2B based on method 1 (blue dots showing RFI mainly over the east coast of the United States).

2) Clean brightness temperature at 23.8GHz is usually higher than that at 18.7GHz. Differences between co-polar measurements centered at 18.7GHz and 23.8GHz are used to detect RFI. Figure 4 shows the RFI map of 18.7GHz obtained by this method.

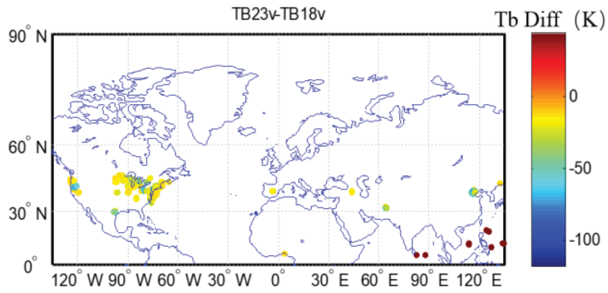

Figure 4. RFI Index at K band derived from HY-2B based on method 2 (yellow and green dots showing RFI mainly over the east coast of the United States).

There is reasonable concordance between the two sets of results. Both maps in Figure 3 and 4 show RFI appearing over the east coast of the United States.

RFI affects brightness temperature differently with different center frequency, bandwidth and resolution. The center frequency of HY-2B in K band is at 18.7GHz, while SSMIS works at 19.35GHz. Figure 5(a) and (b) illustrate differences of brightness temperature in the same region acquired from these two instruments. Analyzing results of HY-2B shows that, the regions influenced by RFI is red circled at around 41°N, 78°W. The measurements of SSMIS indicate the same place is free from RFI. Therefore, to reduce RFI contamination, it's essential to choose reasonable center frequency and bandwidth.

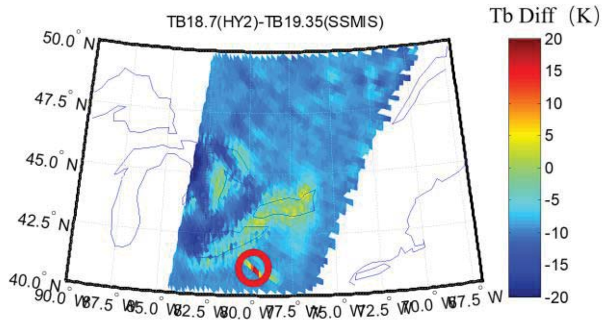

(a)

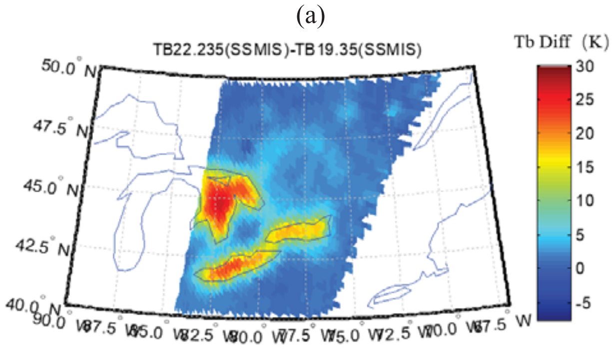

(b)

Figure 5. Differences of brightness temperature in the same region acquired from HY-2B and SSMIS (a) differences of brightness temperature between HY-2B and

SSMIS; (b) differences of brightness temperature between two channels of SSMIS (red line circles RFI at around 41°N, 78°W in HY-2B, while measurements of SSMIS indicate the same place is free from RFI).

2.3 Lessons Learnt from HY-2B RFI Activities

Moderate and strong RFI in C and K band can be easily detected by comparing spectral difference. Future work will concentrate more on low RFI emissions and RFI reflected by sea. In order to reduce RFI contamination, it's essential to choose reasonable center frequency and bandwidth for future mission.

3 Preliminary RFI Studies for the Chinese Ocean Salinity Satellite

The Chinese Ocean Salinity Satellite will carry a two-dimensional IMR. Preliminary studies to detect contaminated observations for synthetic aperture interferometric microwave radiometers has been carried out, and a precise way for RFI localization has been proposed and tested on real IMR images.

3.1 RFI detecting method for IMR

The most intuitive way to detect and flag RFI sources is to find the outliers that are higher than normal brightness temperature. Previous studies have been carried out on SMOS based on such idea, and works well with strong RFI. Focusing on weaker RFIs, we propose a statistical method based on kurtosis and skewness.

Kurtosis and skewness are statistical measures used to describe flatness and asymmetry in a distribution. The kurtosis k of a distribution x can be defined as the fourth moment around the mean divided by the square of the variance of the probability distribution, while skewness s is the third moment around the mean divided by the cube of standard deviation.

$$k = \frac{E(x-\mu)^4}{\sigma^4} \tag{3}$$

$$s = \frac{E(x-\mu)^3}{\sigma^3} \tag{4}$$

where μ is the mean of x, σ is the standard deviation of x, and $E(x)$ represents the expected value of the quantity x.

A normal distribution has a kurtosis of 3. Shown in Figure 6(a), distributions with positive kurtosis have heavier tails, while distributions with negative kurtosis have lighter tails. Figure 6(b) shows density of probability x with different skewness. The skewness of the normal distribution is zero. Negative skew refers to a longer or fatter tail on the left, while positive skew refers to a longer or fatter tail on the right.

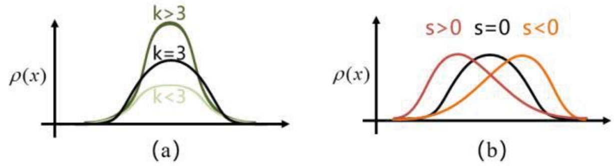

Figure 6. Different distributions with different kurtosis and skewness (a) kurtosis; (b) skewness.

By utilizing all pixels, kurtosis and skewness measure outliers in statistical level, which is RFI in our case. Low RFI emissions, sometimes also give contribution to change in density of probability. Therefore, it is possible to detect weaker RFI sources.

RFI sources, ranging from 30K to 300K are added to the model of clean scene, and the missed detections are listed in Table 1. With RFI emissions grow stronger, missed detections gradually reduce to 0.

Table 1.
Missed Detections of Different RFIs

Strength of RFI	Missed Detection
30K	2.8369%
60K	1.7730%
90K	0.7092%
120~300K	0

3.2 RFI localizing method for IMR[6]

The effects of the RFI source in IMR are in the form of high resolution oscillations. Consider a disk T_D of radius r centered on RFI source:

$$T_D = \{(\xi,\eta):(\xi-\xi_0)^2+(\eta-\eta_0)^2 \le r^2\} \tag{5}$$

and let R_D be the local range (max difference) of T_D in the disk:

$$R_D = \max(T_D) - \min(T_D) \tag{6}$$

The variations of R_D for the scene with the RFI source stick to those for the RFI source only. Therefore, parameters of the RFI emitter can be estimated from R_D, derived from data of the scene with the RFI source like it would be done with the same quantity derived from inaccessible data of the RFI source only.

The idea is therefore to minimize R_D in the vicinity of the RFI emitter. Experiments have been carried out in anechoic chamber. A Y-shaped interferometric array fitted with 10 equally spaced antennas is used for imaging. Figure 7 shows the antenna array.

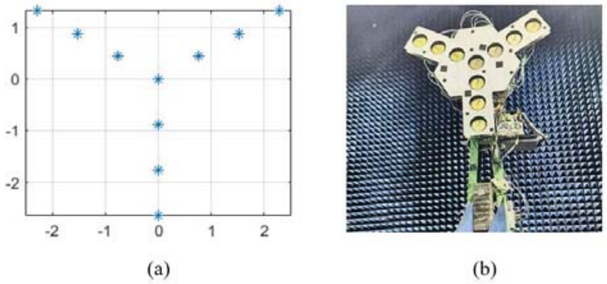

Figure 7. Y-shaped interferometric array used for RFI localization (a) antenna arrangement; (b) interferometric array.

Three snapshots are shown in Figure 8. The RFI emitters are located at (-0.2412,0), (-0.0989,0) and (0.2412,0) respectively. The first column (a), (c), and (e), shows the corresponding Tb reconstructed by DFT imaging. The known RFI locations are marked with red circles. The second column (b), (d), and (f), are the local range of the disk centered at each pixel. The local minima are marked with red circles as well. Table 2 shows specific results of the RFI localization, and the distance in direction. The angle span of one pixel is about 7.54°, and the ratios of localization error to pixel are listed in the last row. The localization accuracy can reach sub-pixel level.

Table 2.
Specific results of the RFI localization

Results	Snapshot1	Snapshot2	Snapshot3
True	(-0.2412,0)	(-0.0989,0)	(0.2412,0)
RFI localization	(-0.2482,0)	(-0.1064,0)	(0.2482,0)
Distance in direction	0.4136°	0.4320°	0.4136°
Ratio	0.0549	0.0573	0.0549

4 Conclusion

In this work, we present current RFI detecting method based on spectral difference in HY-2B. RFI appears over continental areas in Asia, America, Africa and Australia. In order to reduce RFI contamination, it's essential to choose reasonable center frequency and bandwidth for future mission.

The Salinity Satellite of China will carry a two-dimensional Interferometric Microwave Radiometer (IMR). Preliminary studies to detect contaminated observations based on statistical characteristics has been carried out. Missed detection for 90K RFI can be reduced to 0.7092%. A precise way for RFI localization has been proposed and tested on real IMR images. The localization accuracy can reach sub-pixel level.

5 References

1 Yan Li et al., "Analysis of the Antenna Array Orientation Performance of the Interferometric Microwave Radiometer (IMR) Onboard the Chinese Ocean Salinity Satellite," *Sensors*, **20**, 5396, September 2020, doi: 10.3390/s20185396.

2 R. Oliva et al., "SMOS radio frequency interference scenario: Status and actions taken to improve the RFI environment in the 1400–1427 MHz passive band," *IEEE Transactions on geoscience and remote sensing*, **50**, 5, May 2012, pp. 1427–1439, doi: 10.1109/TGRS.2012.2182775.

4 David Draper, David Newell, "An assessment of radio frequency interference using the GPM microwave imager," *IGARSS* 2015, pp. 5170-5173, doi: 10.1109/IGARSS.2015.7326998.

5 Darren McKague et al., "Characterization of k-band radio frequency interference from AMSR-E Windsat and SSM/I" *IGARSS* 2010, pp. 2492-2494, doi: 10.1109/IGARSS.2010.5651860.

6 He Ren et al., "A Precise Localization of RFI Sources in Synthetic Aperture Interferometric Radiometers," *UCMMT* 2020, doi: 10.1109/UCMMT49983.2020.9296104.

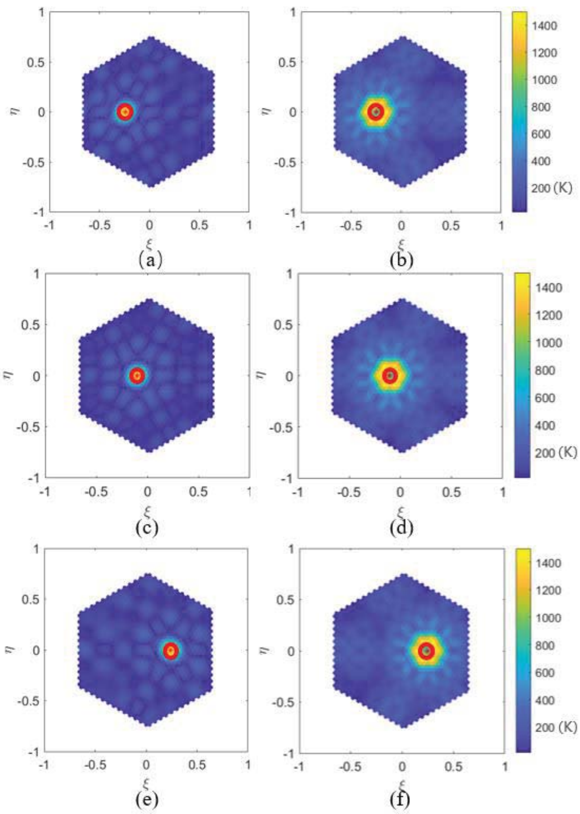

Figure 8. Results of RFI localization. The first column (a), (c), and (e), shows the corresponding BTs reconstructed by DFT imaging. The known RFI locations are marked with red circles. The second column (b), (d), and (f), are the local range of the disk centered at each pixel. The local minima are marked with red circles as well.